$$b_{jk}, b_{ik}^{U}, b_{ik}^{L}, Q_{ijk}^{U}, Q_{ijk}^{L}, C_j \in \{0,1\} \quad (21)$$

4. RESULTS AND DISCUSSION

The hyperbox classification algorithm using the novel MILP framework of Tan et al. (2020) generated rule-based decision models for the CFRP retrofitted RC beams. During the data processing, the dataset was divided into two groups: training (60%) and validation (40%). Each training setup gave results for the two CFRP configurations under investigation (i.e., side-bond and U-wrap). The format of the rule-based decision models (representing one hyperbox each) which determines safe composite systems are as follows:

IF $x_1^L \leq i_1 \leq x_1^U$ **AND** $x_2^L \leq i_2 \leq x_2^U \ldots$ **AND** $x_N^L \leq i_N \leq x_N^U$ **THEN** $V_f = 1$

False positives and negatives have critical implications for both the composite systems and the model predictions. Thus, their corresponding rough translations are given below. Type 1 errors, or false positives, pose severe threats in structural retrofitting considering the brittle nature of shear failure; hence, it is treated as the critical misclassification error in this study.

Type 1 error (false positive): The beam is identified as adequately strengthened in shear by the EB CFRP, but it is actually not sufficiently strengthened.
Type 2 error (false negative): The beam is identified as inadequately strengthened in shear by the EB CFRP, but it is actually sufficiently strengthened.

The first set of rules was generated to minimize the false negatives (γ) while keeping the false positives (ω) less than 0. The summary of the lower and upper bounds for the side-bonded and U-wrapped CFRP is shown in Table 2.

Table 2. Boundaries for the parameters under Rule 1.

Parameter	Unit	Side-bonded		U-wrapped	
		X_i^L	X_i^U	X_i^L	X_i^U
f_c'	MPa	22.2	61.0	24.9	35.0
a/d	-	1.19	3.20	1.50	5.02
ρ_s	-	-	0.003	-	0.008
ρ_L	-	0.012	0.040	0.021	0.048
ρ_{FRP}	-	0.0010	0.0222	0.0007	0.0019
d_f	mm	107.5	417.1	285.0	482.6
ε_u	%	7.7	19.2	10.4	20.7

The results for Rule 1 indicate that the rule applies to all retrofitted beams regardless of the internal transverse reinforcements. After the dimensions have been obtained through the training phase, the model will undergo the validation phase. The

prediction performances of the models for the validation phase, through the dimensions of "actual" and "predicted", are shown in confusion matrices. Results show that 13 of 13 safe retrofitted beams and 4 of 13 unsafe retrofitted beams were correctly identified, as summarized in the following confusion matrices (Table 3 and Table 4). Sample calculations to determine the false positives (ω_V) and false negatives (γ_V) are given as follows. These calculations are valid for all succeeding confusion matrix calculations.

Type 1 errors / false positives of the validation group (ω_V) for Rule 1 (side-bonded):

$$\omega_V = \frac{4-4}{4} = 0.000$$

Type 2 errors / false negatives of the validation group (γ_V) for Rule 1 (side-bonded):

$$\gamma_V = \frac{22-13}{22} = 0.409$$

Type 1 errors / false positives of the validation group (ω_V) for Rule 1 (U-wrapped):

$$\omega_V = \frac{15-14}{15} = 0.067$$

Type 2 errors / false negatives of the validation group (γ_V) for Rule 1 (U-wrapped):

$$\gamma_V = \frac{7-1}{7} = 0.857$$

Table 3. Confusion matrix for side-bond CFRP using Rule 1 ($\omega_V = 0.000;\ \gamma_V = 0.409$).

N = 26	Actual safe	Actual unsafe
Predicted safe	13	0
Predicted unsafe	9	4

Table 4. Confusion matrix for U-wrap CFRP using Rule 1 ($\omega_V = 0.067;\ \gamma_V = 0.857$).

N = 22	Actual safe	Actual unsafe
Predicted safe	1	1
Predicted unsafe	6	14

The second set of rules was generated with the objective of minimizing the false positives (ω) while keeping the false negatives (γ) less than 0. The summary of the lower and upper bounds for the side-bonded and U-wrapped CFRP is shown in Table 5. A model configured to minimize false negatives generally yields more conservative results, which are ideal to generate V_f values that would render composite systems safe. The corresponding confusion matrices are given in Table 6 and Table 7.

Table 5. Boundaries for the parameters under Rule 2.

Parameter	Unit	Side-bonded		U-wrapped	
		X_i^L	X_i^U	X_i^L	X_i^U
f_c'	MPa	22.5	71.4	16.7	39.2
a/d	-	1.22	3.20	1.50	5.00
ρ_s	-	-	0.008	-	0.008
ρ_L	-	0.005	0.040	0.011	0.037
ρ_{FRP}	-	0.0002	0.0267	0.0005	0.0028
d_f	mm	110.0	500.0	153.1	542.9
ε_u	%	7.7	19.2	10.5	20.7

Table 6. Confusion matrix for side-bond CFRP using Rule 2 ($\omega_V = 0.000;\ \gamma_V = 0.455$).

N = 26	Actual safe	Actual unsafe
Predicted safe	12	0
Predicted unsafe	10	4

Table 7. Confusion matrix for U-wrap CFRP using Rule 2 ($\omega_V = 0.333;\ \gamma_V = 0.571$).

N = 22	Actual safe	Actual unsafe
Predicted safe	3	5
Predicted unsafe	4	10

Multiple hyperboxes can also be utilized to explore other decision models, which may yield higher accuracies. This scenario can be executed by changing the predefined number of hyperboxes through the MILP framework. The logical disjunction “OR” is also added in the decision model for every hyperbox created.

Table 8. Boundaries for the parameters under Rule 3.

Group	Parameter	Unit	Side-bonded		U-wrapped	
			X_i^L	X_i^U	X_i^L	X_i^U
Box 1	f_c'	MPa	22.2	71.7	22.4	32.8
	a/d	-	1.19	3.13	1.50	5.02
	ρ_s	-	-	0.008	-	0.008
	ρ_L	-	0.014	0.040	0.017	0.048
	ρ_{FRP}	-	0.0012	0.0118	0.0007	0.0008
	d_f	mm	112.6	500.0	253.1	542.9
	ε_u	%	15.0	19.3	10.5	20.6
Box 2	f_c'	MPa	22.2	70.7	16.4	50.7
	a/d	-	1.22	3.20	3.20	4.98
	ρ_s	-	-	0.008	-	0.008
	ρ_L	-	0.005	0.037	0.010	0.032
	ρ_{FRP}	-	-	0.0267	0.0004	0.0022
	d_f	mm	107.5	500.0	200.0	416.9
	ε_u	%	7.6	17.0	15.0	20.7

A possible disadvantage is the added complexity to the algorithm, which may result in the generation of a slower or unattainable result. Nevertheless, this study adopts a two-hyperbox approach to the two CFRP configurations set to minimize false positives while keeping false negatives less than 0.

Table 9. Confusion matrix for side-bond CFRP using Rule 3 ($\omega_V = 0.000;\ \gamma_V = 0.545$).

N = 26	Actual safe	Actual unsafe
Predicted safe	10	0
Predicted unsafe	12	4

Table 10. Confusion matrix for U-wrap CFRP using Rule 3 ($\omega_V = 0.000;\ \gamma_V = 0.857$).

N = 22	Actual safe	Actual unsafe
Predicted safe	1	0
Predicted unsafe	6	15

The accuracy must be assessed to determine the best-performing models for each configuration. The value for accuracy is given by Eq. (22) and the respective training accuracies for each model are given in Table 11. The results indicate that the best performing models for the two CFRP configurations are Rule 1 (side-bonded) and Rule 3 (U-wrapped) with the highest accuracies at 65.38% and 100.00%, respectively.

$$Accuracy = \frac{True\ Positive + True\ Neative}{Total\ Samples} \tag{22}$$

Table 11. Accuracy yields for the rule-based models.

No. of Hyperboxes	Rule	Configuration	Training Objective	Accuracy, %
One	**Rule 1**	**S-bonded**	**Minimize $\gamma,\ \omega < 0$**	**65.38**
	Rule 1	U-wrapped	Minimize $\gamma,\ \omega < 0$	68.18
	Rule 2	S-bonded	Minimize $\omega,\ \gamma < 0$	61.54
	Rule 2	U-wrapped	Minimize $\omega,\ \gamma < 0$	59.09
Two	Rule 3	S-bonded	Minimize $\omega,\ \gamma < 0$	53.85
	Rule 3	**U-wrapped**	**Minimize $\omega,\ \gamma < 0$**	**100.00**

Assessment of the best-performing models was done with 52 retrofitted RC beams. It should be noted that these beams are different from those analyzed by the ML program. The configurations were split into 44% for the s-bonded CFRP and 56% for the U-wrapped CFRP, accounting for 23 and 29 beams, respectively. Table 12 and Table 13 summarize the corresponding performances of the best-performing models of each CFRP configuration. A red cell indicates that a sample is outside the boundaries for the said parameter. The sample must be within limits across all characteristics to be predicted safe (i.e., assigned a model value of 1). The μ is then assessed using

$V_{f,theoretical}$ values based on ACI and *fib 14*. A sample is concluded to be accurately predicted if the model prediction matches the respective μ value of the design code.

Table 12. Performances of governing model for side-bonded CFRP vs. design codes.

Ref	Parameters							Model	Design Code		Conclusion	
	$f'c$	a/d	ρ_s	ρ_L	ρ_{FRP}	d_f	ε_u		ACI	*fib*	ACI	*fib*
Ma et al. 2020	37.4	1.88	0.001	0.006	0.0003	300.0	21.3	unsafe	unsafe	unsafe	correct	correct
	37.4	1.88	0.001	0.006	0.0006	300.0	21.3	unsafe	unsafe	unsafe	correct	correct
Beber and Campos Filho 2005	32.8	2.84	0.000	0.031	0.0007	300.0	14.8	unsafe	safe	safe	wrong	wrong
	32.8	2.84	0.000	0.031	0.0007	300.0	14.8	unsafe	safe	safe	wrong	wrong
	32.8	2.84	0.000	0.031	0.0007	300.0	14.8	unsafe	safe	safe	wrong	wrong
	32.8	2.84	0.000	0.031	0.0015	300.0	14.8	safe	safe	safe	correct	correct
	32.8	2.84	0.000	0.031	0.0015	300.0	14.8	safe	safe	safe	correct	correct
	32.8	2.84	0.000	0.031	0.0093	300.0	12.2	safe	unsafe	unsafe	wrong	wrong
	32.8	2.84	0.000	0.031	0.0066	300.0	12.2	safe	unsafe	unsafe	wrong	wrong
Salama et al. 2019	47.2	2.16	0.010	0.006	0.0136	100.0	21.0	unsafe	safe	unsafe	wrong	correct
	47.2	2.16	0.010	0.006	0.0272	100.0	21.0	unsafe	safe	unsafe	wrong	correct
	47.2	2.16	0.010	0.006	0.0136	150.0	21.0	unsafe	unsafe	unsafe	correct	correct
	47.2	2.16	0.010	0.006	0.0272	150.0	21.0	unsafe	unsafe	unsafe	correct	correct
	47.2	2.16	0.010	0.006	0.0136	50.0	21.0	unsafe	unsafe	unsafe	correct	correct
	47.2	2.16	0.010	0.006	0.0272	50.0	21.0	unsafe	safe	unsafe	wrong	correct
Allam and Ebeido 2003	40.0	2.57	0.003	0.029	0.0011	200.0	15.2	safe	safe	safe	correct	correct
	40.0	2.57	0.003	0.029	0.0011	200.0	15.2	safe	safe	safe	correct	correct
	40.0	2.57	0.003	0.029	0.0011	200.0	15.2	safe	safe	safe	correct	correct
	40.0	2.57	0.003	0.029	0.0022	200.0	15.2	safe	safe	safe	correct	correct
	40.0	2.57	0.003	0.029	0.0022	200.0	15.2	safe	safe	safe	correct	correct
	40.0	2.57	0.003	0.029	0.0022	200.0	15.2	safe	safe	safe	correct	correct
	40.0	1.71	0.003	0.029	0.0011	200.0	15.2	safe	safe	safe	correct	correct
	40.0	1.71	0.003	0.029	0.0022	200.0	15.2	safe	safe	safe	correct	correct

Table 13. Performances of governing model for U-wrapped CFRP vs. design codes.

Ref	Parameters							Model	Design Code		Conclusion	
	$f'c$	a/d	ρ_s	ρ_L	ρ_{FRP}	d_f	ε_u		ACI	*fib*	ACI	*fib*
Ma et al. 2020	37.4	1.88	0.001	0.006	0.0003	300.0	21.3	unsafe	unsafe	unsafe	correct	correct
	37.4	1.88	0.001	0.006	0.0006	300.0	21.3	unsafe	unsafe	unsafe	correct	correct
Beber and Campos Filho 2005	32.8	2.84	0.000	0.031	0.0007	300.0	14.8	safe	safe	safe	correct	correct
	32.8	2.84	0.000	0.031	0.0007	300.0	14.8	safe	safe	safe	correct	correct
	32.8	2.84	0.000	0.031	0.0007	300.0	14.8	safe	safe	safe	correct	correct
	32.8	2.84	0.000	0.031	0.0007	300.0	14.8	safe	safe	safe	correct	correct
	32.8	2.84	0.000	0.031	0.0007	300.0	14.8	safe	safe	safe	correct	correct
	32.8	2.84	0.000	0.031	0.0005	300.0	14.8	unsafe	safe	safe	wrong	wrong
	32.8	2.84	0.000	0.031	0.0005	300.0	14.8	unsafe	safe	safe	wrong	wrong
	32.8	2.84	0.000	0.031	0.0015	300.0	14.8	unsafe	safe	safe	wrong	wrong
	32.8	2.84	0.000	0.031	0.0015	300.0	14.8	unsafe	unsafe	safe	correct	correct
Alzate et al. 2013	24.5	3.49	0.001	0.021	0.0023	420.0	16.7	unsafe	unsafe	unsafe	correct	correct
	30.7	3.49	0.001	0.021	0.0014	420.0	16.7	unsafe	unsafe	unsafe	correct	correct
	30.2	3.49	0.001	0.021	0.0013	420.0	15.8	unsafe	unsafe	unsafe	correct	correct
	30.2	3.49	0.001	0.021	0.0013	420.0	15.8	unsafe	unsafe	unsafe	correct	correct
	20.5	3.49	0.001	0.021	0.0008	420.0	15.8	unsafe	unsafe	unsafe	correct	correct
	30.7	3.49	0.001	0.021	0.0008	420.0	15.8	safe	unsafe	unsafe	wrong	wrong
Jayapra-Kash et al 2008	27.4	2.50	0.000	0.017	0.0008	340.0	16.5	unsafe	unsafe	unsafe	correct	correct
	27.4	2.50	0.000	0.017	0.0008	340.0	16.5	unsafe	safe	safe	wrong	wrong
	27.4	2.50	0.000	0.011	0.0006	340.0	16.5	unsafe	unsafe	unsafe	correct	correct
	16.7	4.00	0.000	0.017	0.0008	340.0	16.5	safe	safe	safe	correct	correct
	16.7	4.00	0.000	0.017	0.0008	340.0	16.5	safe	safe	safe	correct	correct
	16.7	4.00	0.000	0.011	0.0008	340.0	16.5	safe	unsafe	unsafe	wrong	wrong
	16.7	4.00	0.000	0.011	0.0008	340.0	16.5	safe	unsafe	unsafe	wrong	wrong
	16.7	4.00	0.000	0.011	0.0008	340.0	16.5	safe	unsafe	unsafe	wrong	wrong
Norris et al. 1997	36.5	2.57	0.002	0.018	0.0315	203.0	11.4	unsafe	unsafe	unsafe	correct	correct
	36.5	2.57	0.002	0.018	0.0315	203.0	11.4	unsafe	unsafe	unsafe	correct	correct
	36.5	2.57	0.002	0.018	0.0315	203.0	11.8	unsafe	unsafe	unsafe	correct	correct
	36.5	2.57	0.002	0.018	0.0236	203.0	8.7	unsafe	unsafe	unsafe	correct	correct

A 3D visualization of the hyperboxes on two parameter axes can be done to assess samples like those found in Table 12 and Table 13. The blue boxes in Figure 1 represent the hyperboxes following the dimenions of the governing models. For example, the governing model for the side-bonded CFRP is Rule 1 (Table 2), and the concrete compressive strength follows the range $[22.2 \leq f_c' \leq 61.0]$. When the sample is inside the hyperbox concerning all the parameters, it is predicted safe. Conversely, when a sample is outside of the the hyperbox for at least one parameter, then it is predicted unsafe. Samples predicted to be safe are marked green, while those indicated as unsafe are marked red. The following example shows a visualiazation of a retrofitted RC beam predicted unsafe using the sample from Ma et al (2020) (first sample indicated in Table 12) shown in Figure 1. The sample is indicated by the yellow arrows.

Visualizations in ML assessment, though uncommon, play an important role especially in research and structural engineering. A primary function of 3D visualization is to provide decision-makers (e.g., engineers) a graphical view of any occurring trends concerning the hyperbox dimensions. This functionality may provide new insights on the influential parameters determined or the rule-based models generated (e.g., many samples fail the overall criteria due to certain parameter/s).

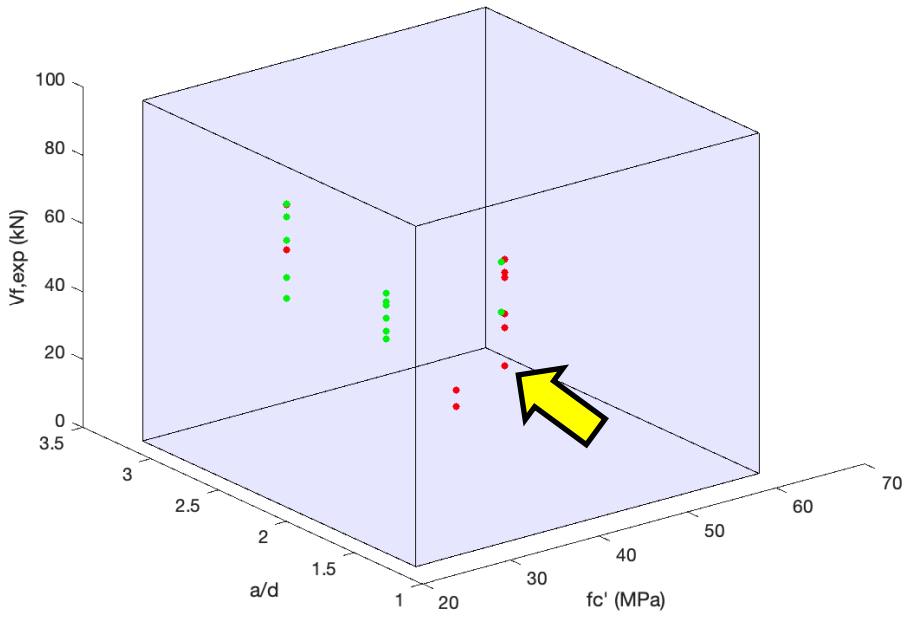

(a) point is within boundary of f_c' and a/d

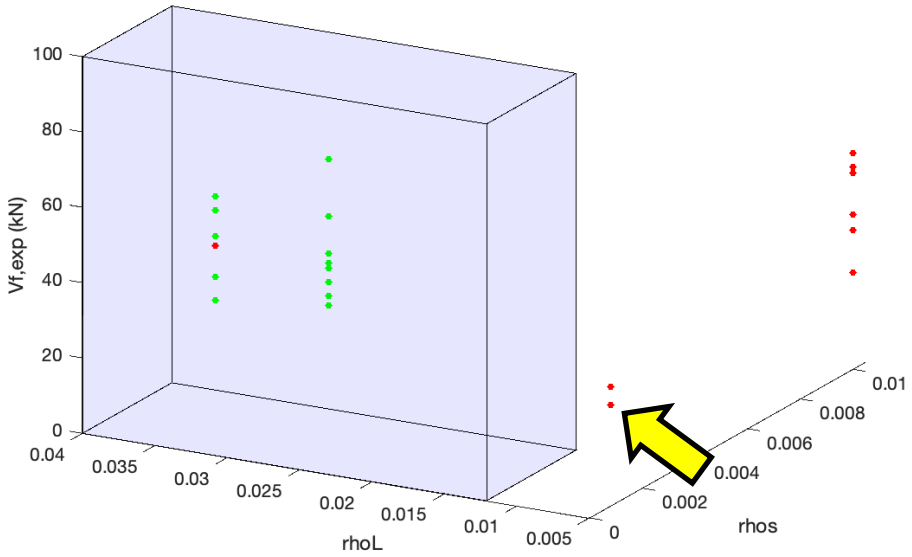

(b) point is within boundary of ρ_s but not ρ_L

Figure 1. 3D visualualization of the side bonded CFRP beam sample (Ma et al) predicted as unsafe by the model.

The rule-based models produced in this study gave satisfactory results concerning similar studies reviewed (Abuodeh et al 2020; Zhou et al 2020; Kar et al 2021). A summary of the performances is given in Figure 2. The results of the governing hyperbox model for the S-bonded CFRP yielded 18 of 23 (or 78%) and 15 of 23 (or 65%) correct predictions using the *fib 14* and ACI, respectively. Meanwhile, the results of the governing hyperbox model for the U-wrapped CFRP yielded 21 of 29 (or 72%) and 22 of 29 (or 76%) correct predictions using the *fib 14* and ACI, respectively.

The discrepancies between the figure above and the results from the validation phase illustrate several limitations of the MILP-based hyperbox classification modeling approach. One limitation is being unable to yield the same degree of accuracy consistently. This limitation can partially be attributed to the limited samples that the MILP can process to determine a global optimum. Another limitation is the non-consideration of external factors in constructing this database. Only parameters explicitly given in the references (or required only minimal calculations and assumptions) were further processed to enhance the likelihood of producing an accurate model.

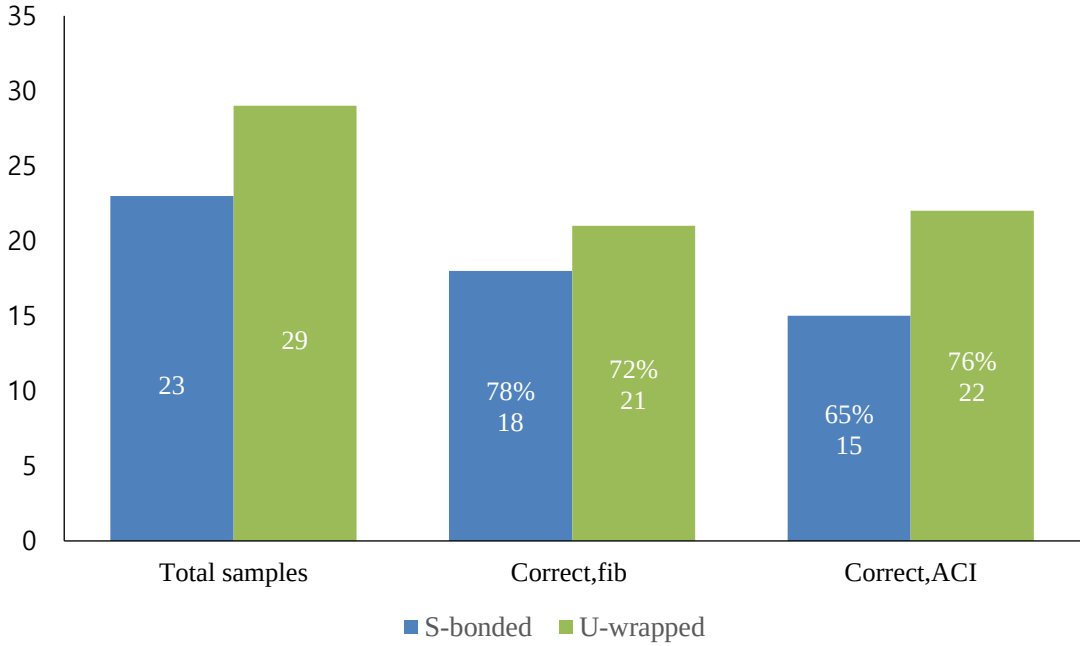

Figure 2. Performance summary of governing rule-based models.

5. CONCLUSIONS AND RECOMMENDATIONS

The produced rule-based equations showcase an ML application with hyperboxes using a novel MILP approach. The work presented serves as an example of solving problems requiring binary decisions for critical but ambiguous scenarios. False positive (or Type 1) occurrences are considered the critical errors in this scenario. The best-performing models determine if the composite CFRP-RC systems are safe based on the shear contribution (V_f) of the EB CFRP. This study analyzed only side-bonded and U-wrapped CFRP on simply supported beams. The processed data from the combined samples reveal that there are seven influential parameters determining V_f of the EB CFRP. The governing models yielded accuracies of 65.38% and 100.0% for the side-bonded and U-wrapped CFRP, respectively, and mitigated the occurrence of false positives during the validation phase. The governing models yielded accurate predictions of 78% (S-bonded) and 72% (U-wrapped) with *fib 14* and 65% (S-bonded) and 76% (U-wrapped) with ACI. The rule-based hyperbox models generated provided a feature of minimizing misclassification errors during their creation phase, translating to minimal prediction errors in actual applications. Therefore, a marked advantage for the hyperbox models is demonstrated over the capabilities of existing design codes. Overall, the models can serve as decision guidelines amidst the uncertainties in complex behaviors like shear mechanics.

Nevertheless, improvements can be made by future research to improve the accuracy yields of the best-performing rule-based models. One possibility is to try different frameworks aside from MILP for classifying samples. Another recommendation

is to derive closed-form solutions to analyze the effects of the parameters in determining the sufficiency of CFRP shear contribution.

REFERENCES

Abuodeh, O. R., Abdalla, J. A., & Hawileh, R. A. (2020). Prediction of shear strength and behavior of RC beams strengthened with externally bonded FRP sheets using machine learning techniques. Composite Structures, 234, 111698.

ACI Committee 440, & Busel, J. P. (2008). Specification for carbon and glass fiber-reinforced polymer bar materials for concrete reinforcement. American Concrete Institute.

Adhikari, S. (2009). Mechanical properties and flexural applications of basalt fiber reinforced polymer (BFRP) bars (Doctoral dissertation, University of Akron).

Akroush, N., Almahallawi, T., Seif, M., & Sayed-Ahmed, E. Y. (2017). CFRP shear strengthening of reinforced concrete beams in zones of combined shear and normal stresses. Composite Structures, 162, 47-53.

Al-Mahaidi, R., & Kalfat, R. (2018). Rehabilitation of concrete structures with fiber-reinforced polymer. Butterworth-Heinemann.

Al-Saawani, M. A., El-Sayed, A. K., & Al-Negheimish, A. I. (2020). Effect of shear-span/depth ratio on debonding failures of FRP-strengthened RC beams. Journal of Building Engineering, 32, 101771.

Alhroob, E., Mohammed, M. F., Lim, C. P., & Tao, H. (2019). A critical review on selected fuzzy min-max neural networks and their significance and challenges in pattern classification. IEEE access, 7, 56129-56146.

Amran, Y. M., Alyousef, R., Rashid, R. S., Alabduljabbar, H., & Hung, C. C. (2018, November). Properties and applications of FRP in strengthening RC structures: A review. In Structures (Vol. 16, pp. 208-238). Elsevier.

Aviso, K. B., Demeterio III, F. P. A., Janairo, J. I. B., Lucas, R. I. G., Promentilla, M. A. B., Tan, R. R., & Yu, D. E. C. (2021). What University Attributes Predict for Graduate Employability?. Cleaner Engineering and Technology, 100069.

Azad, C., Mehta, A. K., & Jha, V. K. (2018, July). Improved data classification using fuzzy euclidean hyperbox classifier. In 2018 International Conference on Smart Computing and Electronic Enterprise (ICSCEE) (pp. 1-6). IEEE.

Belarbi, A., & Acun, B. (2013). FRP systems in shear strengthening of reinforced concrete structures. Procedia Engineering, 57, 2-8.

Breña, S. F., Bramblett, R. M., Benouaich, M. A., Wood, S. L., & Kreger, M. E. (2001). Use of carbon fiber reinforced polymer composites to increase the flexural capacity of reinforced concrete beams (No. Research Report 1776-1). University of Texas at Austin.

Ceroni, F., Cosenza, E., Gaetano, M., & Pecce, M. (2006). Durability issues of FRP rebars in reinforced concrete members. Cement and concrete composites, 28(10), 857-868.

Chaabene, W. B., Flah, M., & Nehdi, M. L. (2020). Machine learning prediction of mechanical properties of concrete: Critical review. Construction and Building Materials, 260, 119889.

Chaallal, O., Nollet, M. J., & Perraton, D. (1998). Strengthening of reinforced concrete beams with externally bonded fiber-reinforced-plastic plates: design guidelines for shear and flexure. Canadian Journal of Civil Engineering, 25(4), 692-704.

Chandrakar, J., & Singh, A. K. (2017). Study of Various Local and Global Seismic Retrofitting Strategies—A review. Int. J. Eng. Res. Technol, 6, 824-831.

Chen, G. M., Li, S. W., Fernando, D., Liu, P. C., & Chen, J. F. (2017). Full-range FRP failure behaviour in RC beams shear-strengthened with FRP wraps. International Journal of Solids and Structures, 125, 1-21.

Chen, G. M., Teng, J. G., & Chen, J. F. (2013). Shear strength model for FRP-strengthened RC beams with adverse FRP-steel interaction. Journal of Composites for Construction, 17(1), 50-66.

Chen, J. F., & Teng, J. G. (2003). Shear capacity of fiber-reinforced polymer-strengthened reinforced concrete beams: Fiber reinforced polymer rupture. Journal of Structural Engineering, 129(5), 615-625.
Colotti, V. (2016). Mechanical shear strength model for reinforced concrete beams strengthened with FRP materials. Construction and Building Materials, 124, 855-865.
Das, S. (2011). Life cycle assessment of carbon fiber-reinforced polymer composites. The International Journal of Life Cycle Assessment, 16(3), 268-282.
El-Maaddawy, T., & Chekfeh, Y. (2012). Retrofitting of severely shear-damaged concrete t-beams using externally bonded composites and mechanical end anchorage. Journal of Composites for Construction, 16(6), 693-704.
Godat, A., Labossière, P., & Neale, K. W. (2012). Numerical investigation of the parameters influencing the behaviour of FRP shear-strengthened beams. Construction and Building Materials, 32, 90-98.
Hanoon, A. N., Jaafar, M. S., Hejazi, F., & Aziz, F. N. A. (2017). Strut-and-tie model for externally bonded CFRP-strengthened reinforced concrete deep beams based on particle swarm optimization algorithm: CFRP debonding and rupture. Construction and Building Materials, 147, 428-447.
Huang, Z., Tu, Y., Meng, S., Sabau, C., Popescu, C., & Sas, G. (2019). Experimental study on shear deformation of reinforced concrete beams using digital image correlation. Engineering Structures, 181, 670-698.
Huo, J., Li, Z., Zhao, L., Liu, J., & Xiao, Y. (2018). Dynamic behavior of carbon fiber-reinforced polymer-strengthened reinforced concrete beams without stirrups under impact loading. ACI Structural Journal, 115(3), 775-787.
John, K., & Naidu, S. V. (2004). Tensile properties of unsaturated polyester-based sisal fiber–glass fiber hybrid composites. Journal of Reinforced Plastics and Composites, 23(17), 1815-1819.
Kar, S., Pandit, A. R., & Biswal, K. C. (2021). A neuro-fuzzy approach to estimate the shear contribution of externally bonded FRP composites. Asian Journal of Civil Engineering, 22(2), 351-367.
Karzad, A. S., Leblouba, M., Al Toubat, S., & Maalej, M. (2019). Repair and strengthening of shear-deficient reinforced concrete beams using Carbon Fiber Reinforced Polymer. Composite Structures, 223, 110963.
Khalifa, A., Gold, W. J., Nanni, A., & MI, A. A. (1998). Contribution of externally bonded FRP to shear capacity of RC flexural members. Journal of composites for construction, 2(4), 195-202.
Khuat, T. T., Ruta, D., & Gabrys, B. (2021). Hyperbox-based machine learning algorithms: a comprehensive survey. Soft Computing, 25(2), 1325-1363.
Landesmann, A., Seruti, C. A., & Batista, E. D. M. (2015). Mechanical properties of glass fiber reinforced polymers members for structural applications. Materials Research, 18(6), 1372-1383.
Lavorato, D., Nuti, C., & Santini, S. (2018). Experimental investigation of the shear strength of RC beams extracted from an old structure and strengthened by carbon FRP U-strips. Applied Sciences, 8(7), 1182.
Lee, D. H., Kim, K. S., Han, S. J., Zhang, D., & Kim, J. (2018). Dual potential capacity model for reinforced concrete short and deep beams subjected to shear. Structural Concrete, 19(1), 76-85.
Lee, J. Y., Hwang, H. B., & Doh, J. H. (2012). Effective strain of RC beams strengthened in shear with FRP. Composites Part B: Engineering, 43(2), 754-765.
Li, W., & Leung, C. K. (2016). Shear span–depth ratio effect on behavior of RC beam shear strengthened with full-wrapping FRP strip. Journal of Composites for Construction, 20(3), 04015067.
Lütjering, G., & Williams, J. C. (2007). Titanium. Springer Science & Business Media.
Ma, S., Muhamad Bunnori, N., & Choong, K. K. (2020). Experimental study on shear strengthening of reinforced concrete box beam by CFRP. Iranian Journal of Science and Technology, Transactions of Civil Engineering, 44(4), 1075-1085.
Mansouri, I., Kisi, O., Sadeghian, P., Lee, C. H., & Hu, J. W. (2017). Prediction of ultimate strain and strength of FRP-confined concrete cylinders using soft computing methods. Applied Sciences, 7(8), 751.

Meier, U. (1991). Strengthening of structures with CFRP. In Advanced Composite Materials in Civil Engineering Structures, Proc. Specialty Conf. Las Vegas, NV (pp. 224-232). ASCE.

Mhanna, H. H., Hawileh, R. A., & Abdalla, J. A. (2019). Shear strengthening of reinforced concrete beams using CFRP wraps. Procedia Structural Integrity, 17, 214-221.

Miller, T. C., Chajes, M. J., Mertz, D. R., & Hastings, J. N. (2001). Strengthening of a steel bridge girder using CFRP plates. Journal of bridge engineering, 6(6), 514-522.

Mostofinejad, D., & Kashani, A. T. (2013). Experimental study on effect of EBR and EBROG methods on debonding of FRP sheets used for shear strengthening of RC beams. Composites Part B: Engineering, 45(1), 1704-1713.

Naderpour, H., & Alavi, S. A. (2017). A proposed model to estimate shear contribution of FRP in strengthened RC beams in terms of Adaptive Neuro-Fuzzy Inference System. Composite Structures, 170, 215-227.

Naser, M. Z., Hawileh, R. A., & Abdalla, J. A. (2019). Fiber-reinforced polymer composites in strengthening reinforced concrete structures: A critical review. Engineering Structures, 198, 109542.

Oller, E., Kotynia, R., & Marí, A. (2021). Assessment of the existing models to evaluate the shear strength contribution of externally bonded FRP shear reinforcements. Composite Structures, 266, 113641.

Ongpeng J., Lecciones I.N., Garduque J.A., Buera D.J. (2020). Ultimate Confined Compressive Strength of Carbon Fiber-Reinforced Circular and Rectangular Concrete Column. In: Alfred R., Lim Y., Haviluddin H., On C. (eds) Computational Science and Technology. Lecture Notes in Electrical Engineering, vol 603. Springer, Singapore. https://doi.org/10.1007/978-981-15-0058-9_34

Pampanin, S., Bolognini, D., & Pavese, A. (2007). Performance-based seismic retrofit strategy for existing reinforced concrete frame systems using fiber-reinforced polymer composites. Journal of Composites for Construction, 11(2), 211-226.

Peng, L., & Stewart, M. G. (2014). Spatial time-dependent reliability analysis of corrosion damage to RC structures with climate change. Magazine of Concrete Research, 66(22), 1154-1169.

Pohoryles, D. A., Melo, J., Rossetto, T., Fabian, M., McCague, C., Stavrianaki, K., ... & Sargeant, B. (2017). Use of DIC and AE for monitoring effective strain and debonding in FRP and FRCM-retrofitted RC beams. Journal of Composites for Construction, 21(1), 04016057.

Qureshi, H. J., & Saleem, M. U. (2018). Flexural and shear strain characteristics of carbon fiber reinforced polymer composite adhered to a concrete surface. Materials, 11(12), 2596.

Salama, A. S. D., Hawileh, R. A., & Abdalla, J. A. (2019). Performance of externally strengthened RC beams with side-bonded CFRP sheets. Composite Structures, 212, 281-290.

Saleem, M. U., Qureshi, H. J., Amin, M. N., Khan, K., & Khurshid, H. (2019). Cracking behavior of RC beams strengthened with different amounts and layouts of CFRP. Applied Sciences, 9(5), 1017.

Sarasini, F., Tirillò, J., Ferrante, L., Valente, M., Valente, T., Lampani, L., ... & Sorrentino, L. (2014). Drop-weight impact behaviour of woven hybrid basalt–carbon/epoxy composites. Composites Part B: Engineering, 59, 204-220.

Schmidt, M., Schmidt, P., Wanka, S., & Classen, M. (2021). Shear Response of Members without Shear Reinforcement—Experiments and Analysis Using Shear Crack Propagation Theory (SCPT). Applied Sciences, 11(7), 3078.

Siddika, A., Al Mamun, M. A., Ferdous, W., & Alyousef, R. (2020). Performances, challenges and opportunities in strengthening reinforced concrete structures by using FRPs-A state-of-the-art review. Engineering Failure Analysis, 104480.

Simpson, P. K. (1992). Fuzzy min—max neural networks—Part 1: Classification. IEEE Trans. on Neural Networks, 3(5), 776-786.

Singh, S. B. (2013). Shear response and design of RC beams strengthened using CFRP laminates. International Journal of Advanced Structural Engineering, 5(1), 1-16.

Song, Y. Y., & Ying, L. U. (2015). Decision tree methods: applications for classification and prediction. Shanghai archives of psychiatry, 27(2), 130.
Tan, R. R., Aviso, K. B., Janairo, J. I. B., & Promentilla, M. A. B. (2020). A hyperbox classifier model for identifying secure carbon dioxide reservoirs. Journal of Cleaner Production, 272, 122181.
Triantafillou, T. C. (1998). Shear strengthening of reinforced concrete beams using epoxy-bonded FRP composites. ACI structural journal, 95, 107-115.
Xu, G., & Papageorgiou, L. G. (2009). A mixed integer optimisation model for data classification. Computers & Industrial Engineering, 56(4), 1205-1215.
Zadeh, L. A. (1965). Fuzzy sets. Information and control, 8(3), 338-353.
Zhou, Y., Zhang, J., Li, W., Hu, B., & Huang, X. (2020). Reliability-based design analysis of FRP shear strengthened reinforced concrete beams considering different FRP configurations. Composite Structures, 237, 111957.